

See discussions, stats, and author profiles for this publication at: <https://www.researchgate.net/publication/225041532>

Nuclear magnetic resonance J coupling constant polarizabilities of hydrogen peroxide: A basis set and correlation study

ARTICLE in JOURNAL OF COMPUTATIONAL CHEMISTRY · SEPTEMBER 2012

Impact Factor: 3.59 · DOI: 10.1002/jcc.23013 · Source: PubMed

CITATIONS

6

READS

12

6 AUTHORS, INCLUDING:



Gabriel I Pagola

National Scientific and Technical Research C...

18 PUBLICATIONS 93 CITATIONS

SEE PROFILE



Marta B Ferraro

University of Buenos Aires

111 PUBLICATIONS 1,479 CITATIONS

SEE PROFILE



Stephan P. A. Sauer

University of Copenhagen

179 PUBLICATIONS 3,572 CITATIONS

SEE PROFILE

Nuclear Magnetic Resonance J Coupling Constant Polarizabilities of Hydrogen Peroxide: A Basis Set and Correlation Study

Hanna Kjær,^[a] Monia R. Nielsen,^[a] Gabriel I. Pagola,^[b] Marta B. Ferraro,^[b] Paolo Lazzeretti,^[c] and Stephan P. A. Sauer*^[a]

In this article, we present the so far most extended investigation of the calculation of the coupling constant polarizability of a molecule. The components of the coupling constant polarizability are derivatives of the nuclear magnetic resonance (NMR) indirect nuclear spin–spin coupling constant with respect to an external electric field and play an important role for both chiral discrimination and solvation effects on NMR coupling constants. In this study, we illustrate the effects of one-electron basis sets and electron correlation both at the level of density functional theory as well as second-order polarization propagator approximation for the small molecule

hydrogen peroxide, which allowed us to perform calculations with the largest available basis sets optimized for the calculation of NMR coupling constants. We find a systematic but rather slow convergence with the one-electron basis set and that augmentation functions are required. We observe also large and nonsystematic correlation effects with significant differences between the density functional and wave function theory methods. © 2012 Wiley Periodicals, Inc.

DOI: 10.1002/jcc.23013

Introduction

Nuclear magnetic resonance (NMR) spectroscopy is the most important experimental technique for determining the structure of molecules in solution. However, currently available NMR spectrometers are unable to determine the absolute configuration of a chiral molecule in solution, as the chemical shifts and spin–spin coupling constants (SSCCs) are exactly the same for the two enantiomers of a chiral molecule, if parity violation contributions^[1–4] are neglected. Chiral discrimination, that is, the recognition of different enantiomers, is so far only possible with NMR-based methods when chiral reagents or solvents are added.^[5,6] However, recent articles suggest that chirality could actually be observable in NMR spectroscopy through application of an electric field, whose effect is in principle detectable via especially designed experimental setups.^[7–11]

For the case of the indirect nuclear SSCC, the response property involved is referred to as electric polarizability of the indirect nuclear spin–spin coupling,^[8,11–13] that is, a third-rank tensor even under time-reversal and odd under parity, having components with the same magnitude but opposite sign for *D* and *L* enantiomers of a chiral species. In crystal phase, all the polarizability components are possibly observable. In liquid and gas phase, a pseudoscalar, $\bar{J}_{IJ}^{(1)}$, of the SSCC polarizability of coupled nuclei *I* and *J* can be defined^[8,14,15] via spatial averaging^[16] of the polarizability. The pseudoscalar vanishes in achiral molecules and has equal but opposite values for the two enantiomers of a chiral molecule in disordered media.

The individual components of the SSCC polarizability and in particular the vector of electric field derivatives of the isotropic SSCC^[12,13] with components A_{α}^{IJ} are not directly measurable in

NMR experiments in disordered media but play an important role for the description of environment effects on SSCC.^[13]

Nevertheless, the electric-dipole polarizability of indirect nuclear spin–spin coupling has received much less attention than the corresponding nuclear magnetic shielding polarizability.^[7–11,17–32] The first article by Grayson^[12] presented coupled perturbed Hartree–Fock (HF) and second-order polarization propagator (SOPPA) calculations for the polarizabilities of the geminal proton–proton coupling in CH₃F, CH₃Cl, CH₃Br, CH₃I, CH₄, CH₃Li, CH₃Na, and CH₃K using standard energy optimized basis sets of at most valence triple zeta quality. It was followed by the proposal of Buckingham and Fischer^[8] that, also for the nuclear spin–spin coupling polarizability tensor, a pseudoscalar can be defined. Preliminary density functional theory (DFT) calculations on (2R)-2-methyloxirane, (*R_d*)-1,3-dimethylallene, and (2R)-*N*-methyloxaziridine using the B3LYP, KT3, and PBE functionals indicate that the magnitude of this pseudoscalar is very small,^[14,15] which would make chiral discrimination quite difficult via currently available NMR techniques. However, like in the first study, the basis sets used in these calculations are not particularly optimized for the calculation of coupling constants

[a] H. Kjær, M. R. Nielsen, S. P. A. Sauer
Department of Chemistry, University of Copenhagen, Universitetsparken 5,
DK-2100 Copenhagen Ø, Denmark
E-mail: sauer@kiku.dk

[b] G. I. Pagola, M. B. Ferraro
Departamento de Física, Facultad de Ciencias Exactas y Naturales,
Universidad de Buenos Aires and IFIBA, CONICET, Ciudad Universitaria,
Pabellón 1, (1428) Buenos Aires, Argentina

[c] P. Lazzeretti
Dipartimento di Chimica dell'Università degli Studi di Modena e Reggio
Emilia, Via Campi 183, 41124 Modena, Italy

© 2012 Wiley Periodicals, Inc.

or coupling constant polarizabilities. Finally, in the recent exploration of a multipole SSCC polarizability/reaction field approach to solvation,^[13] the basis set dependence of the polarizability and hyperpolarizability of the one-bond nitrogen–hydrogen coupling constant in *N*-methylacetamide was investigated at the DFT/B3LYP level. It was found that standard energy optimized basis sets are not suitable and that specialized SSCC basis set like, for example, the pcJ-n and aug-pcJ-n basis sets^[33,34] ought to be used. Consequently, to our knowledge, no systematic correlation and basis set study using not only DFT but also correlated wave function methods has so far been presented for the SSCC polarizability and its pseudoscalar $\bar{J}_U^{(1)}$.

This article aims therefore at investigating one-electron basis set, electron correlation, and geometry effects for the indirect nuclear spin–spin coupling polarizability. To be able to use the largest available SSCC basis sets not only in the DFT but also in correlated wave function calculations, we had to restrict ourselves to a rather small, chiral molecule. We choose therefore to study hydrogen peroxide.

Theory

The total energy of a molecule W in the presence of an external time independent and spatially uniform electric field \mathbf{E} and intramolecular perturbations due to the permanent magnetic dipoles \mathbf{m}_I at the nuclei, can be written as^[35]:

$$W = W^{(0)} + \sum_{\alpha\beta} m_{I\alpha} K_{\alpha}^{I\alpha J\beta} m_{J\beta} + \sum_{\alpha\beta\gamma} m_{I\alpha} K_{\alpha}^{I\alpha J\beta} m_{J\beta} E_{\gamma} + \dots \quad (1)$$

Within the Born–Oppenheimer philosophy, the nuclear magnetic dipoles $\mathbf{m}_I = \gamma_I \mathbf{I}_I$ and $\mathbf{m}_J = \gamma_J \mathbf{I}_J$ are merely perturbative parameters, expressed via the magnetogyric ratios γ_I and γ_J , and spins \mathbf{I}_I and \mathbf{I}_J of two coupled nuclei I and J . The reduced nuclear spin–spin coupling in the absence of an electric field is represented by a second-rank tensor,

$$K_{\alpha}^{I\alpha J\beta} = \left. \frac{\partial^2 W}{\partial m_{I\alpha} \partial m_{J\beta}} \right|_{\mathbf{m}_I, \mathbf{m}_J, \mathbf{E} \rightarrow \mathbf{0}}, \quad (2)$$

and the polarizability of nuclear spin–spin coupling is a third-rank tensor, obtained as the third derivative of the energy, Eq. (1),

$$K_{\alpha}^{I\alpha J\beta} = \left. \frac{\partial^3 W}{\partial m_{I\alpha} \partial m_{J\beta} \partial E_{\gamma}} \right|_{\mathbf{m}_I, \mathbf{m}_J, \mathbf{E} \rightarrow \mathbf{0}}. \quad (3)$$

Therefore, the reduced nuclear spin–spin coupling tensor in the presence of an applied electric field can be expanded in a Taylor series as:

$$K_{\alpha}^{I\alpha J\beta}(E) = K_{\alpha}^{I\alpha J\beta} + \sum_{\gamma} K_{\alpha}^{I\alpha J\beta} E_{\gamma} + \dots \quad (4)$$

where $K_{\alpha}^{I\alpha J\beta}(\mathbf{0}) \equiv K_{\alpha}^{I\alpha J\beta}$.

The reduced coupling tensor components are related to those of the $J^{I\alpha J\beta}$ tensor commonly expressed in Hertz by

$$K_{\alpha}^{I\alpha J\beta} = 4\pi^2 \frac{J^{I\alpha J\beta}}{h\gamma_I\gamma_J}. \quad (5)$$

with an analogous relationships for the coupling polarizability

$$K_{\alpha}^{I\alpha J\beta} = 4\pi^2 \frac{J_{\alpha}^{I\alpha J\beta}}{h\gamma_I\gamma_J}, \quad (6)$$

The isotropic SSCC measured in NMR spectra corresponds then to one-third of the trace of this tensor

$$J^U = \frac{1}{3} \sum_{\alpha} J^{I\alpha J\alpha} \quad (7)$$

Two averages of the SSCC polarizability will be considered in the following. The first

$$A_{\alpha}^{IJ} = \frac{1}{3} \sum_{\alpha} J_{\alpha}^{I\alpha J\alpha} \quad (8)$$

is the vector of electric field derivatives of the isotropic coupling constant^[12,13,23] while the second

$$\bar{J}_U^{(1)} = \frac{1}{6} \sum_{\alpha\beta\gamma} \varepsilon_{\alpha\beta\gamma} J_{\alpha}^{I\alpha J\beta} \quad (9)$$

is the pseudoscalar, which vanishes for achiral molecules but is in principle measurable for chiral molecules even in disordered media.

The elements of the SSCC polarizability are quadratic response functions with the exception of the terms depending on the diamagnetic spin-orbit (DSO) operator, which are only linear response functions as outlined in our previous paper.^[14,15]

The indirect nuclear SSCC arises due to two mechanisms.^[36] In the first, the nuclear spin interacts with the spin magnetic moment of the electrons that gives rise to the Fermi-contact (FC) and spin-dipolar (SD) contributions to the coupling constants and their polarizabilities, whereas in the second, the nuclear spin interacts with the orbital magnetic moments leading to a paramagnetic and a diamagnetic contribution, called the paramagnetic spin-orbit (PSO) and the DSO terms.

Computational Details

Methods and basis sets

The electronic structure methods used in this study for the calculation of NMR indirect nuclear SSCCs and their electric field derivatives, the coupling constant polarizabilities, are coupled perturbed HF, coupled perturbed DFT in combination with the B97-2^[37] and B3LYP^[38–40] exchange–correlation functionals and the three SOPPA-methods: SOPPA,^[41,42] SOPPA(CC2),^[43,44] and SOPPA(CCSD).^[45,46] In the HF and DFT calculations, we have used the pcJ-n and aug-pcJ-n basis sets of Jensen^[33] in the new contraction,^[34] which are specially optimized for accurate calculations of indirect nuclear SSCCs at the DFT-level, for the SOPPA-methods we used the corresponding ccJ-pVXZ basis sets,^[47] which are optimized for calculation of coupling constants at the coupled cluster level, as well as the aug-ccJ-pVXZ basis sets, which are the ccJ-pVXZ basis sets augmented with

the diffuse functions of the corresponding aug-cc-pVXZ. We also used the aug-cc-pVTZ-J basis sets,^[46,48–53] which are optimized for calculating coupling constants dominated by the FC-term. All calculations have been performed using the Dalton 2011 program.^[54]

Derivatives

Although the field-free coupling constant tensor elements have been calculated as linear response functions,^[43,46,55,56] the electric field derivatives at the SOPPA, SOPPA(CC2), and SOPPA(CCSD) level have been calculated numerically. For the first derivative of an element of the coupling constant tensor with respect to an electric field, the following two-point formula has been used

$$J_{\gamma}^{I_2 J_{\beta}} = \frac{J_{\gamma}^{I_2 J_{\beta}}(+E_{\gamma}) - J_{\gamma}^{I_2 J_{\beta}}(-E_{\gamma})}{2E_{\gamma}}, \quad (10)$$

where E is the field strength and $J_{\gamma}^{I_2 J_{\beta}}(+E_{\gamma})$ is an element of the coupling constant tensor calculated in the presence of an electric field. Based on test calculations as discussed below, we used in all production calculations a field strength of 0.001 au.

At the DFT level, the components of the J coupling polarizability can alternatively be obtained as numerical derivatives of the coupling constant or analytically as linear (the DSO contribution) or quadratic (the PSO, SD, and FC contributions) response functions.^[14,15] This allows for an additional check of the accuracy of our numerical derivative scheme.

Molecular geometry

The molecular equilibrium geometry of H_2O_2 adopted in the calculations has been optimized at the DFT/B3LYP/6-31G* level using the Dalton 2011 program.^[54] For the series of rotamers, corresponding to different HO–OH dihedral angles, the remaining geometrical parameters have been kept fixed at the equilibrium geometry values. In the equilibrium geometry, the two oxygen atoms were placed along the y -axis with the z -axis intersecting the dihedral angle as shown in Figure 1.

Results and Discussion

Accuracy of the numerical derivatives

To estimate the errors which we may introduce by calculating the coupling constant derivatives numerically, we performed several test calculations at the coupled HF level using the aug-pcJ-1 basis set. First, we tested the effect of changing the convergence criteria in the solution of the HF and coupled HF equations, from the default values, 10^{-5} and 10^{-3} , to 10^{-10} and 10^{-6} , respectively. The first derivatives with respect to the electric field were changed by less than 0.1 Hz/au. Consequently, we use the default convergence criteria in the production calculations. Second, we tested the two-point formula Eq. (10). We calculated the coupling constant for seven different field strengths (–0.01 au, –0.001 au, –0.0001 au, 0 au, 0.0001 au, 0.001 au, and 0.01 au), and fitted these to a fifth-order polynomial. Compared with this fit, the largest error obtained

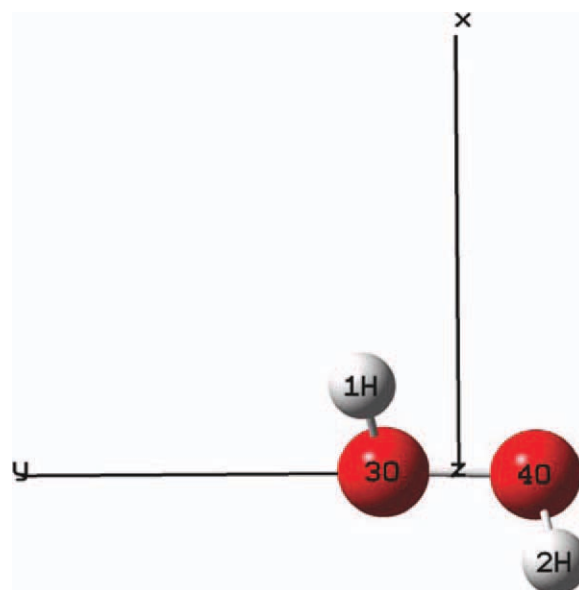


Figure 1. Placement of the coordinate axes (y -axis to the left and x -axis upward) relative to the atoms for the equilibrium geometry. [Color figure can be viewed in the online issue, which is available at wileyonlinelibrary.com.]

with the two-point formula, Eq. (10), is for the derivative in x -direction of the one-bond $J_{\text{O}_3\text{H}_1}$ coupling, where we observe an error of –2 Hz/au, which is less than 0.5%. Finally, we have compared the results of the numerical calculations using the two-point formula to analytical results obtained using linear and quadratic response function and found that all deviations are less than 0.1 Hz/au. Corresponding small deviations are observed at the B3LYP/aug-pcJ-3 level between the two-point formula and analytical calculations. Consequently, we can expect our derivatives calculated by the two-point formula to be of sufficient accuracy.

Basis set effects

In the study of the basis set dependence of the HF and DFT results, we used the pcJ- n and aug-pcJ- n series of basis sets as well as the aug-cc-pVTZ-J basis set, whereas for the three SOPPA-methods, we used the ccJ-pVXZ and aug-ccJ-pVXZ basis sets. We will only discuss the DFT/B97-2 and SOPPA(CCSD) results in detail here, as both the other HF/DFT and the other SOPPA methods exhibit corresponding basis set dependence as can be seen from the Supporting Information Tables 1S–16S and 17S–28S.[†] Furthermore, we will not discuss the basis set dependence of the coupling constants themselves in detail, but only summarize that B97-2 results with deviations of 1% or less from the results with the largest basis set, aug-

[†]See Supporting Information for Tables with all the results of the basis set study for the total coupling constant, its derivatives and the pseudoscalar as well as for a figure with the dependence of the derivatives of the one-bond $J_{\text{O}_3\text{H}_1}$ coupling on the dihedral angle calculated using DFT/B97-2 and the aug-pcJ-3 basis set.

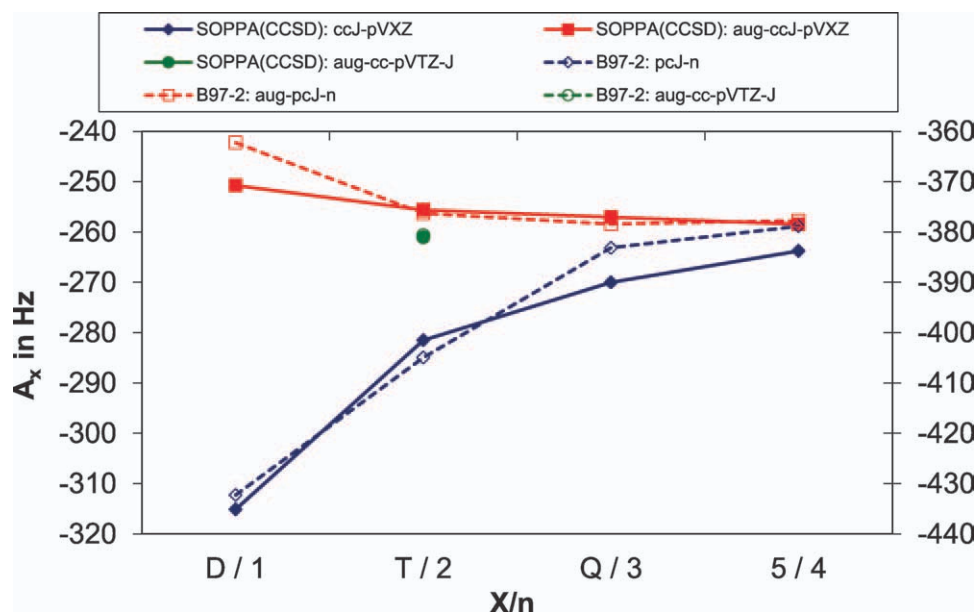


Figure 2. The basis set convergence of the first derivatives with respect to an electric field in x-direction, $A_x^{O_3H_1}$, in Hz/au of the one-bond $J^{O_3H_1}$ coupling at the SOPPA(CCSD)/(aug)-ccJ-pVXZ level (solid lines and left, primary y-axis) and B97-2/(aug)-pcJ-n level (dotted lines and right, secondary y-axis). [Color figure can be viewed in the online issue, which is available at wileyonlinelibrary.com.]

pcJ-4, can be obtained with the (aug)-pcJ-3, pcJ-4 and aug-cc-pVTZ-J basis sets. The latter shows again^[57,58] that for coupling constants dominated by the FC term, the aug-cc-pVTZ-J basis sets can reproduce DFT results from much larger basis sets. Similarly, we find that SOPPA(CCSD) results, which differ by 1% or less from the corresponding aug-ccJ-pV5Z result, can be obtained with the ccJ-pV5Z, (aug)-ccJ-pVQZ, aug-ccJ-pVTZ, and aug-cc-pVTZ-J basis sets.

However, we can see a much larger effect of additional augmentation functions in the SOPPA(CCSD) calculations than in corresponding DFT/B97-2 calculations and can therefore recommend to use in general the augmented version of the ccJ-pVXZ basis sets.

Turning now to the basis set dependence of the coupling constant derivatives, we will illustrate it for the derivatives of the one-bond $J^{O_3H_1}$ coupling constant, which is the largest of the coupling constants in H_2O_2 , and has the largest coupling constant polarizability. The result of the basis set study for these derivatives can be seen in Figures 2–4, while the results for the derivatives of the other three couplings are given in Supporting Information Tables 15–285

results for all three derivatives are only obtained with the aug-ccJ-pVQZ at the wave function level or with the pcJ-4, aug-pcJ-2, and aug-pcJ-3 basis sets at the DFT level. If differences up to 3% are acceptable, also the ccJ-pV5Z, aug-ccJ-pVTZ, and the smaller aug-cc-pVTZ-J basis sets can be used in the wave function calculations or the pcJ-3 and again the smaller aug-cc-pVTZ-J basis sets in DFT calculations. This implies that

(See page footnote on page 3). For both methods, DFT/B97-2 and SOPPA(CCSD), we observe that the results obtained with the original basis sets, pcJ-n and ccJ-pVXZ, increase with increasing n and X , while in the series of augmented basis sets, aug-pcJ-n and aug-ccJ-pVXZ, we observe that the results decrease from $X = D$ to $X = 5$ and from $n = 1$ to $n = 3$, but almost insignificantly increase again from aug-pcJ-3 to aug-pcJ-4 similar to the coupling constant itself. Furthermore, the results obtained with the aug-cc-pVTZ-J basis set are very close to the results from the largest basis sets and differ by only 2–3 Hz/au, which corresponds to less than 1% for $A_x^{O_3H_1}$ and $A_z^{O_3H_1}$ and up to 3% for $A_y^{O_3H_1}$. In general, we observe that differences smaller than ~1% from the largest basis set

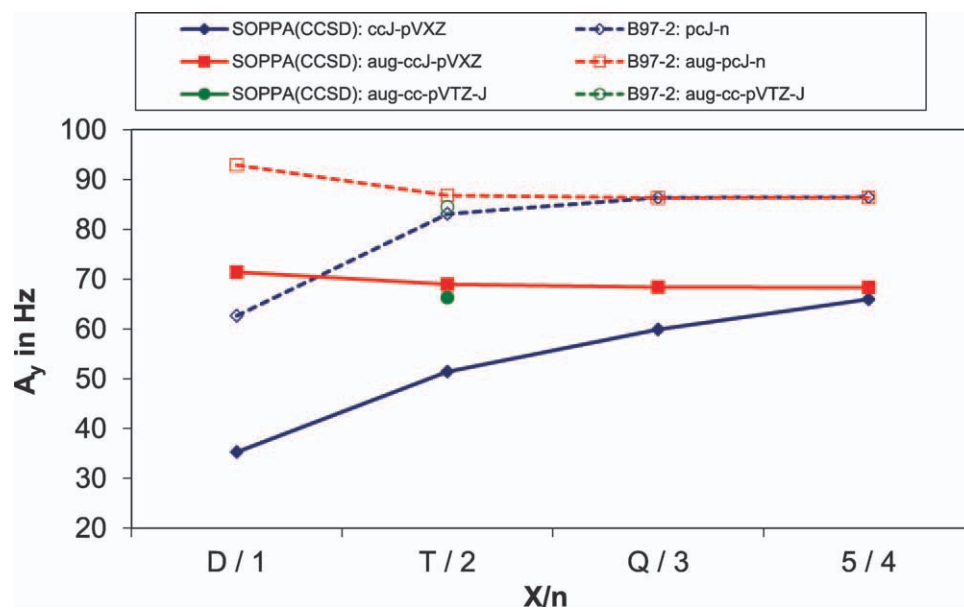


Figure 3. The basis set convergence of the first derivatives with respect to an electric field in y-direction, $A_y^{O_3H_1}$, in Hz/au of the one-bond $J^{O_3H_1}$ coupling at the SOPPA(CCSD)/(aug)-ccJ-pVXZ level (solid lines) and B97-2/(aug)-pcJ-n level (dotted lines). [Color figure can be viewed in the online issue, which is available at wileyonlinelibrary.com.]

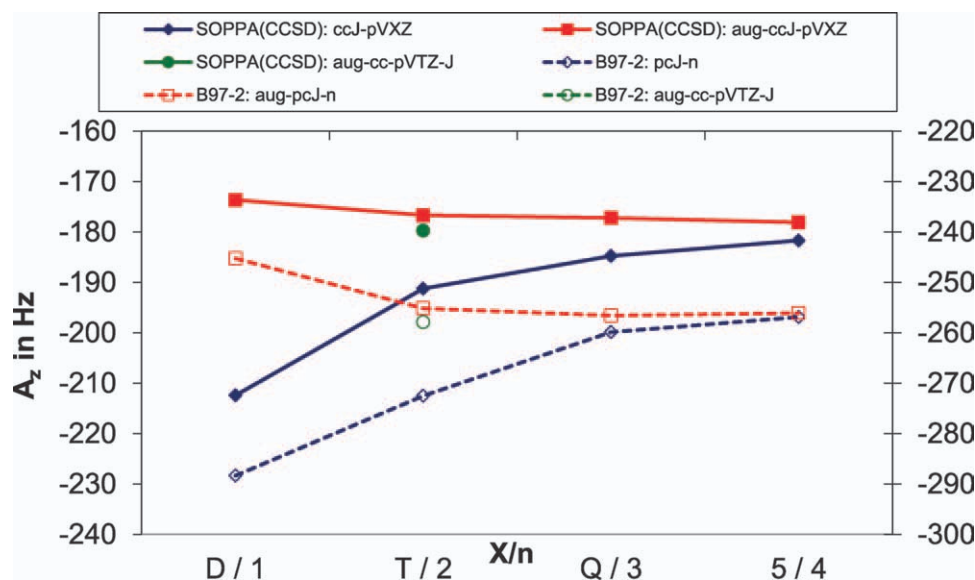


Figure 4. The basis set convergence of the first derivatives with respect to an electric field in z-direction, $A_z^{O_3H_1}$, in Hz/au of the one-bond $J^{O_3H_1}$ coupling at the SOPPA(CCSD)/(aug)-ccJ-pVXZ level (solid lines and left, primary y-axis) and B97-2/(aug)-pcJ-n level (dotted lines and right, secondary y-axis).

inclusion of the augmentation functions in the aug-pcJ-n and aug-ccJ-pVXZ basis sets is even more important for the calculation of the coupling constant polarizabilities, $A_x^{O_3H_1}$, $A_y^{O_3H_1}$, and $A_z^{O_3H_1}$, than for the coupling constant $J^{O_3H_1}$ in good agreement with earlier findings for *N*-methylacetamide at the DFT/(aug)-pcJ-n level.^[13]

In the following analysis of electron correlation effects, we will therefore use the largest basis sets, aug-pcJ-4 and aug-ccJ-pV5Z, but use the smaller basis sets, aug-pcJ-3 and aug-ccJ-pVQZ, for the study of the dihedral angle dependence of the coupling constant polarizabilities.

Electron correlation effects

In this section, the effects of using different functionals or different versions of the SOPPA methods on the calculated coupling constant polarizabilities are discussed. The results for all couplings are given in the Supporting Information (See page footnote on page 3). Here, we will illustrate the conclusion for

Table 1. The one-bond $J^{O_3H_1}$ coupling constant in Hz, its derivatives with respect to an electric field in the *x*-, *y*-, and *z*-direction, and the pseudoscalar $\tilde{J}_{O_3H_1}^{(1)}$ in Hz/au, calculated with different methods using the aug-pcJ-4 basis set for HF and DFT and the aug-ccJ-pV5Z basis set for the three SOPPA-methods.

	aug-pcJ-4			aug-ccJ-pV5Z		
	HF	B3LYP	B97-2	SOPPA	SOPPA(CC2)	SOPPA(CCSD)
$J^{O_3H_1}$	-99.49	-61.32	-59.36	-72.99	-72.34	-71.27
$A_x^{O_3H_1}$	-469.3	-435.2	-377.8	-359.8	-256.1	-258.5
$A_y^{O_3H_1}$	187.0	78.04	86.37	75.35	66.25	68.35
$A_z^{O_3H_1}$	-316.1	-293.3	-256.1	-242.6	-176.2	-178.1
$\tilde{J}_{O_3H_1}^{(1)}$	-2.78	-2.94	-2.69	-2.79	-1.93	-2.02

the isotropic one-bond coupling $J^{O_3H_1}$ and its vector of derivatives with components $A_x^{O_3H_1}$, $A_y^{O_3H_1}$, and $A_z^{O_3H_1}$. These results are collected in Table 1 and are illustrated in Figure 5.

A comparison with experimental values is not possible for this system and unrelaxed coupled cluster calculations of coupling constant polarizability are, to our knowledge, not possible either. We will therefore take the SOPPA(CCSD) results as our best and reference result for the discussion of the other methods. We believe this to be justified, as SOPPA(CCSD) has in numerous studies been shown to reproduce accurately experimental coupling constants and their geometry dependence for most types of coupling constants.^[43,44,46,48,49,59–68] Only in

the case of one-bond coupling constants between two atoms with several lone pairs have significant deviations from experimental data been observed,^[43,67] which would then also apply to the oxygen–oxygen one-bond coupling of hydrogen peroxide. However, in the same studies, this coupling has been calculated at both the CCSD and the three SOPPA levels for various basis sets and no larger differences from the CCSD results than a couple of Hz were observed.

Contrary to the SSCC (Table 1) there is no clear trend with respect to the performance of different methods for the derivatives of the coupling constant (Fig. 5). A similar observation has previously been made for *N*-methylacetamide.^[13] However, with the exception of SOPPA(CC2), all the other methods studied here overestimate the absolute values of the derivatives compared to SOPPA(CCSD). Apart from that the two largest components, $A_x^{O_3H_1}$ and $A_z^{O_3H_1}$, of the vector of derivatives of the isotropic coupling constant show a pattern

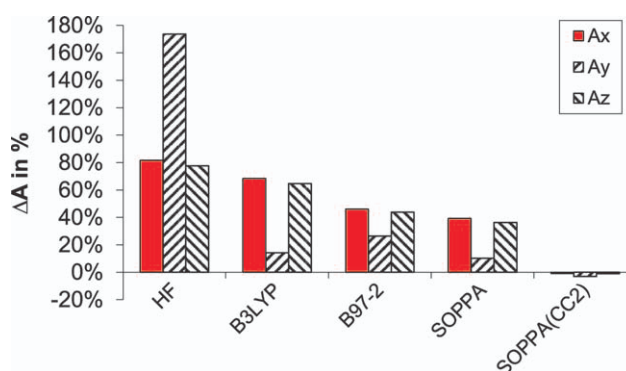


Figure 5. Relative deviations of the derivatives of the one-bond coupling constant $A_x^{O_3H_1}$, $A_y^{O_3H_1}$, and $A_z^{O_3H_1}$ calculated with the different methods from the SOPPA(CCSD) results in %.

that differs from the behavior of the smallest component $A_z^{O_3H_1}$. For the two larger components, HF deviates approximately 80% from the SOPPA(CCSD) results. B3LYP is here inferior to B97-2 that performs almost as good as SOPPA. But, the latter two deviate still by $\sim 40\%$ from the SOPPA(CCSD) results, while SOPPA(CC2) deviates by only 1%, which is a larger improvement of SOPPA(CC2) over SOPPA than seen previously.^[43,44] For the smaller, y-component, we find that apart from HF and SOPPA(CC2), all other methods give smaller relative deviations than for the other two components. Interestingly, it is now B3LYP that is almost as good as SOPPA, both deviating by $\sim 12\%$ from the SOPPA(CCSD) result. Finally, for the pseudoscalar, $\bar{J}_{O_3H_1}^{(1)}$, whose value is with 2 Hz/au about 2 orders of magnitude smaller than the largest components of the coupling constant polarizability, we observe a third pattern, where again SOPPA(CC2) gives clearly the results closest to SOPPA(CCSD), while the other methods give deviations in the range of 33–56% in the order B97-2, SOPPA and HF and finally B3LYP.

Summarizing, we can say that SOPPA(CC2) and SOPPA(CCSD) give almost identical results for the isotropic one-bond coupling $J_{O_3H_1}$ and its derivatives, which in particular for the polarizability significantly differ from the results of the other methods. Concerning the two DFT functionals, B97-2 or B3LYP, it depends on the component, which functional gives the closest agreement with the SOPPA(CCSD) results. For the polarizability, their results are almost equal to the SOPPA results. HF, on the other hand, shows much larger deviations from the other methods, as also found for *N*-methylacetamide.^[13]

Individual contributions to the coupling constant polarizability

In Table 2, the FC, SD, PSO, and DSO contributions to all isotropic coupling constants in H_2O_2 are shown together with the corre-

sponding contributions to the vector (A_x, A_y, A_z) of electric field derivatives of the coupling constants and the pseudoscalar $\bar{J}^{(1)}$. The results were obtained analytically at the DFT/B3LYP level using the aug-pcJ-3 basis set and numerically at the SOPPA(CCSD)/aug-ccJ-pVQZ level. The two methods give quantitatively different results similar to the differences in Table 1 and Figure 5, for example, all components of the coupling constant polarizability are numerically larger at the B3LYP than at the SOPPA(CCSD) level, but qualitatively the same picture appears. For the one- and two-bond coupling constants, the FC term is almost always the largest contribution. However, only in the case of the one-bond oxygen–hydrogen coupling it dominates the total value, while in the two-bond oxygen–hydrogen coupling also the PSO term is almost as large or even larger. In the one-bond oxygen–oxygen coupling finally, even the SD term is almost half as large as the FC term, as is often observed for one-bond couplings between atoms with many lone pairs.^[43,46,49,67,69,70] The vicinal proton–proton coupling constant shows the usual pattern with a PSO and DSO contribution that almost cancel each other, so that the remaining largest contribution is again the FC term.

Let us now turn to the electric field derivatives of the isotropic coupling constants, that is, components of the coupling constant polarizabilities. One notices that due to the symmetry of the molecule only the two heteronuclear couplings have derivatives with respect to fields in all three Cartesian directions and a pseudoscalar $\bar{J}^{(1)}$, while the two homonuclear couplings only are changed to first order by an electric field in z-direction, which is a symmetry axis. This is one of the reasons why we so far have only discussed the one-bond oxygen–hydrogen coupling and its polarizability. In case of the two one-bond coupling constants, always one of the four terms dominates the coupling polarizability. For A_z^{OO} , $A_x^{O_3H_1}$, and $A_z^{O_3H_1}$, this is the FC term while the PSO term is at most

Table 2. The four contributions to the isotropic coupling constants (in Hz), their nonvanishing electric field derivatives (A_x, A_y, A_z) and the nonvanishing pseudoscalar $\bar{J}^{(1)}$ (in Hz/au) of H_2O_2 calculated at the DFT/B3LYP level with the aug-pcJ-3 basis set and at the SOPPA(CCSD) level with the aug-ccJ-pVQZ basis set.

Nuclei	Property	B3LYP/aug-pcJ-3					SOPPA(CCSD)/aug-ccJ-pVQZ				
		FC	SD	PSO	DSO	Total	FC	SD	PSO	DSO	Total
O ₃ –O ₄	J^{OO}	–35.95	14.47	26.79	0.04	5.35	–31.94	12.55	26.81	0.04	7.47
	A_z^{OO}	151.97	1.28	9.22	0.02	162.49	108.60	–3.30	–1.25	0.05	104.10
O ₃ –H ₁	$J_{O_3H_1}^{O_3H_1}$	–57.13	0.14	–4.25	–0.18	–61.42	–68.22	0.29	–3.17	–0.16	–71.25
	$A_x^{O_3H_1}$	–527.34	7.16	81.15	0.97	–438.06	–320.25	2.40	59.85	1.00	–257.05
	$A_y^{O_3H_1}$	–43.03	11.88	107.65	1.34	77.84	–22.75	7.90	81.70	1.60	68.40
	$A_z^{O_3H_1}$	–338.26	4.20	38.40	0.44	–295.22	–206.05	1.15	27.20	0.40	–177.20
	$\bar{J}_{O_3H_1}^{(1)}$	0.00	0.71	2.23	0.01	2.95	—	—	—	—	2.02
	$J_{O_4H_1}^{O_3H_1}$	–4.79	0.79	–4.10	0.35	–7.75	–3.99	0.73	–4.18	0.35	–7.10
O ₄ –H ₁	$A_x^{O_4H_1}$	–15.20	0.74	11.82	–0.05	–2.69	–6.55	0.35	5.90	0.05	–0.25
	$A_y^{O_4H_1}$	34.60	1.86	20.60	–0.10	56.96	44.05	–1.30	13.20	0.15	56.10
	$A_z^{O_4H_1}$	–9.37	1.67	3.65	–0.03	–4.08	–2.55	0.55	2.15	–0.05	0.15
	$\bar{J}_{O_4H_1}^{(1)}$	0.00	0.03	1.32	0.00	1.35	—	—	—	—	2.70
	J^{HH}	1.84	–0.34	5.14	–4.91	1.73	1.64	–0.36	5.20	–4.96	1.52
	A_z^{HH}	–5.76	–0.95	–2.36	–0.13	–9.20	–4.65	–0.75	–1.70	–0.05	–7.10
Tensor components not shown are identical to zero due to the symmetry of the molecule.											

20% of the FC term. But for $A_y^{O_3H_1}$, that is, when the field is parallel to the oxygen–oxygen bond, it is actually the PSO term that is about three times as large as the FC term and about a factor of 10 larger than the nonvanishing SD contribution. The electric field derivatives of the two- and three-bond coupling constants are in general significantly smaller than the corresponding derivatives of the one-bond couplings as mentioned previously with the exception of $A_y^{O_4H_1}$, which is almost as large as $A_y^{O_3H_1}$. Furthermore, the FC term is always the largest contribution to the polarizabilities, although it is at most three times as large as the PSO term. Interestingly, it is again the y-component $A_y^{O_4H_1}$, that is, along the oxygen–oxygen bond, which has the largest PSO term. The pseudoscalars $\bar{J}_{O_3H_1}^{(1)}$ and $\bar{J}_{O_4H_1}^{(1)}$, finally, which consist solely of off-diagonal components of the coupling constant polarizabilities, have therefore no contribution from the isotropic FC. For the two examples studied here, they are clearly dominated by the PSO contribution.

Variation with the dihedral angle

Finally, we have calculated the electric field derivatives and their four contributions for a series of dihedral angles keeping all the other geometrical parameters fixed. We used DFT/B97-2 and SOPPA(CCSD), and will here focus again on the derivatives of the isotropic one-bond oxygen–hydrogen coupling $A_x^{O_3H_1}$, $A_y^{O_3H_1}$, and $A_z^{O_3H_1}$. Although the numerical values for the coupling constant derivatives differ between the DFT/B97-2 and SOPPA(CCSD) calculations, the variation with dihedral angle is almost identical in both methods, and we will therefore only discuss the SOPPA(CCSD) results here in Figures 6–8. The cor-

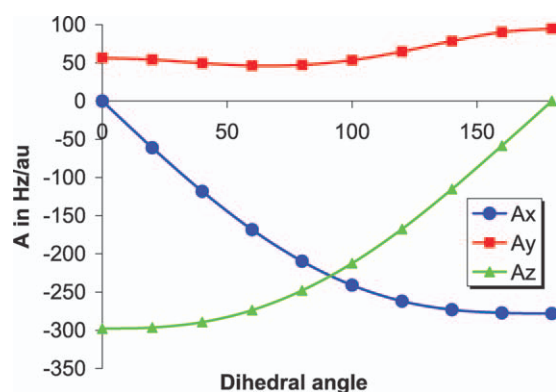


Figure 6. The derivatives of ${}^1J_{O_3H_1}$ for different dihedral angles calculated using SOPPA(CCSD) with the aug-ccJ-pVQZ basis set. [Color figure can be viewed in the online issue, which is available at wileyonlinelibrary.com.]

responding DFT/B97-2 figure is given in Supporting Information Figure 1S (See page footnote on page 3).

In our setup, the two oxygens of H_2O_2 are placed along the y-axis. When the dihedral angle is zero, the molecule is in a *cis*-configuration and the two hydrogens are placed in the yz-plane. For this dihedral angle, the electric field in z-direction is almost parallel to the O–H bonds, while a field in x-direction is completely perpendicular to the O–H bonds. The x-derivative is correspondingly zero for this configuration, while the z-derivative has its largest value. When the dihedral angle is

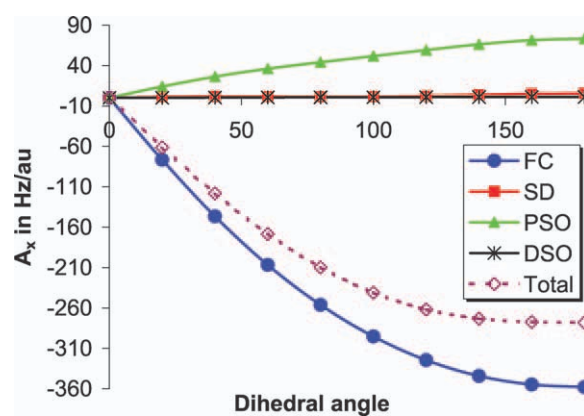


Figure 7. The four contributions to the $A_x^{O_3H_1}$ derivative of ${}^1J_{O_3H_1}$ for different dihedral angles calculated using SOPPA(CCSD) with the aug-ccJ-pVQZ basis set. [Color figure can be viewed in the online issue, which is available at wileyonlinelibrary.com.]

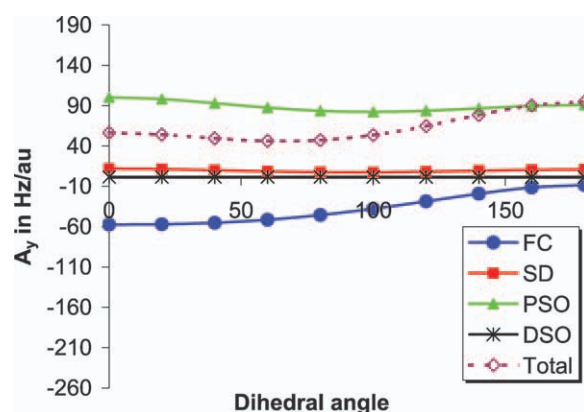


Figure 8. The four contributions to the $A_y^{O_3H_1}$ derivative of ${}^1J_{O_3H_1}$ for different dihedral angles calculated using SOPPA(CCSD) with the aug-ccJ-pVQZ basis set. [Color figure can be viewed in the online issue, which is available at wileyonlinelibrary.com.]

increased, the hydrogens are rotated away from each other into the xy-plane. When the dihedral angle is 180° , the molecule is in a *trans*-configuration with the two hydrogen atoms in the xy-plane. An electric field in x-direction is then almost parallel to the O–H bond, while the electric field in z-direction is perpendicular to the O–H bonds. Correspondingly, it is now the z-derivative which is zero, while the x-derivative has its largest value, which is almost as large as the value of the z-derivative for the *cis*-configuration. At intermediate dihedral angles, both derivatives vary smoothly between their extreme values and adopt the same value at 90° . An electric field in y-direction is for any dihedral angle parallel to the O–O bond and perpendicular to the O–H bonds. The derivative with respect to a field in the y-direction is thus much less affected by changes in the dihedral angle.

Turning now to the four contributions to $A_x^{O_3H_1}$ and $A_y^{O_3H_1}$ in Figures 7 and 8 one can observe first of all that only the FC and PSO terms play a significant role. Second, the changes are dominated by the FC term, whose variation is almost five times as large as the variation of the PSO term in $A_x^{O_3H_1}$ and still 2.5 times as large in $A_y^{O_3H_1}$. However, as the FC and PSO contribution to these coupling polarizability components have opposite signs,

the PSO term is positive while the FC term is negative, and as in case of $A_{yO_3H_1}^{O_3H_1}$, the PSO term is larger than the FC term, the combined effect of the FC and PSO term for the total derivative of the coupling constants is that the variation of the FC term is damped in $A_{xO_3H_1}^{O_3H_1}$ and shifted to positive values in $A_{yO_3H_1}^{O_3H_1}$.

Summary

We have presented for hydrogen peroxide the so far most extended basis set study for the coupling constant polarizability of a molecule, using the largest J-coupling optimized basis sets available, that is, the (aug)-pcJ-n and (aug)-ccJ-pVXZ series. We find that deviations of less than 1% from the largest basis set results can be obtained also with the smaller aug-pcJ-2 and aug-pcJ-3 or the nonaugmented pcJ-4 basis sets at the DFT level and with the aug-ccJ-pVQZ basis sets at the correlated wave function method level. On the other hand, using the nonaugmented pcJ-3 basis set in DFT or the ccJ-pV5Z and aug-ccJ-pVTZ basis sets in wavefunction calculations or the significantly smaller aug-cc-pVTZ-J basis set in both increases the maximum relative deviation to only 3%. We note thus that the performance of the ccJ-pVXZ series of basis sets is significantly improved on adding the augmentation functions of the underlying correlation consistent cc-pVXZ basis sets.

We have studied the effect of electron correlation on the derivatives of the isotropic coupling constants with respect to electric fields using for the first time the correlated wave function methods SOPPA(CCSD) and SOPPA(CC2) in addition to SOPPA and DFT. We observed large correlation effects for the electric field derivatives of the isotropic coupling constants. Uncorrelated coupled HF calculations overestimate the derivatives dramatically, giving values that are almost three times as large for some of the components. SOPPA(CC2), on the other hand, gives results almost indistinguishable from our best, SOPPA(CCSD), results, while larger deviations are already observed also for SOPPA. Concerning the two exchange-correlation functionals B3LYP and B97-2, which are used in the DFT calculations, no clear trend is observed apart from that their results for the derivatives deviate even more than the SOPPA results from the SOPPA(CCSD) values but not as much as the coupled HF results. However, it depends on the direction of the applied electric field, which functional performs better. For a field parallel to the oxygen-oxygen bond, where the PSO term is the dominant contribution to the coupling polarizability, the B3LYP correlation-exchange functional gives results close to the SOPPA values, whereas for the x- and y-components that are strongly dominated by the FC mechanism, the B97-2 functional gives results comparable to SOPPA. We observe thus no general trend with respect to the performance of different exchange-correlation functionals.

For H_2O_2 , we thus note that it is either the PSO or FC mechanisms that is mostly affected by the external electric field, but which one is the main term depends on the coupling and direction of the electric field relative to the molecule. In particular, whether the field is along the oxygen-oxygen bond or perpendicular to it has a large effect on the coupling polarizability.

Finally, the variation of the coupling polarizability with the dihedral angle in H_2O_2 is very much dominated by the FC term even though it might not be the largest contribution to it as in the case of the electric field parallel to the oxygen-oxygen bond.


Concluding from the study on this single model-compound, hydrogen peroxide, we expect that converged calculations of coupling constant polarizabilities require in general even larger basis sets than the underlying coupling constants, in particular sufficient numbers of diffuse functions, and that correlation effects can be large and can differ significantly for the different components of the polarizabilities.

Acknowledgments

S.P.A.S. acknowledges support from the Danish Center for Scientific Computing (DCSC) and the financial support from the Carlsberg Foundation and from the Danish Natural Science Research Council/The Danish Councils for Independent Research (grant number 272-08-0486). H.K. thanks the Natural Science Faculty of University of Copenhagen for a 3-year Ph.D. stipend. Financial support (UBACYT 20020100100105 from the University of Buenos Aires and PIP0369 from CONICET) is gratefully acknowledged.

Keywords: spin-spin coupling constant polarizability · nuclear magnetic resonance · chiral discrimination · basis set · second-order polarization propagator

How to cite this article: H. Kjær, M. R. Nielsen, G. I. Pagola, M. B. Ferraro, P. Lazzeretti, S. P. A. Sauer, *J. Comput. Chem.* **2012**, *33*, 1845–1853. DOI: 10.1002/jcc.23013

 Additional Supporting Information may be found in the online version of this article.

- [1] A. L. Barra, J. B. Robert, *Mol. Phys.* **1996**, *88*, 875.
- [2] J. B. Robert, A. L. Barra, *Chirality* **2001**, *13*, 699.
- [3] G. Laubender, R. Berger, *ChemPhysChem* **2003**, *4*, 395.
- [4] A. Soncini, F. Faglioni, P. Lazzeretti, *Phys. Rev. A* **2003**, *68*, 33402.
- [5] D. Parker, *Chem. Rev.* **1991**, *91*, 1441.
- [6] I. Canet, J. Courtieu, A. Loewenstein, A. Meddour, J. M. Pechine, *J. Am. Chem. Soc.* **1995**, *117*, 6520.
- [7] A. D. Buckingham, *Chem. Phys. Lett.* **2004**, *398*, 1.
- [8] A. D. Buckingham, P. Fischer, *Chem. Phys.* **2006**, *324*, 111.
- [9] R. Zanasi, S. Pelloni, P. Lazzeretti, *J. Comput. Chem.* **2007**, *28*, 2159.
- [10] S. Pelloni, P. Lazzeretti, R. Zanasi, *J. Chem. Theory Comput.* **2007**, *3*, 1691.
- [11] P. Lazzeretti, A. Soncini, R. Zanasi, *Theor. Chem. Acc.* **2008**, *119*, 99.
- [12] M. Grayson, *Int. J. Mol. Sci.* **2003**, *4*, 218.
- [13] H. Kjær, S. P. A. Sauer, J. Kongsted, *J. Comput. Chem.* **2011**, *32*, 3168.
- [14] G. I. Pagola, M. B. Ferraro, S. Pelloni, P. Lazzeretti, S. P. A. Sauer, *Theor. Chem. Acc.* **2011**, *129*, 359.
- [15] G. I. Pagola, M. B. Ferraro, S. Pelloni, P. Lazzeretti, S. P. A. Sauer, *Theor. Chem. Acc.* **2011**, *130*, 127.
- [16] A. D. Buckingham, J. A. Pople, *Proc. Phys. Soc. A* **1955**, *68*, 905.
- [17] W. T. Raynes, J. A. Tossel, In *Nuclear Magnetic Shieldings and Molecular Structure*; J. A. Tossel, Ed.; Kluwer Academic Publisher: Dordrecht, **1993**; pp. 401–420.
- [18] W. T. Raynes, In *Encyclopedia of Magnetic Resonance*; D. M. Grant, R. K. Harris, Eds.; Wiley: Chichester, **1996**; Vol. 3, pp. 1846–1856.
- [19] A. D. Buckingham, *Can. J. Chem.* **1960**, *38*, 300.
- [20] B. Day, A. D. Buckingham, *Mol. Phys.* **1976**, *32*, 343.
- [21] J. P. Riley, W. T. Raynes, *Mol. Phys.* **1976**, *32*, 569.

- [22] A. J. Sadlej, W. T. Raynes, *Mol. Phys.* **1978**, *35*, 101.
- [23] W. T. Raynes, R. Ratcliffe, *Mol. Phys.* **1979**, *37*, 571.
- [24] S. Coriani, A. Rizzo, K. Ruud, T. Helgaker, *Chem. Phys.* **1997**, *216*, 53.
- [25] S. M. Cybulski, D. M. Bishop, *Chem. Phys. Lett.* **1996**, *250*, 471.
- [26] D. M. Bishop, S. M. Cybulski, *Mol. Phys.* **1993**, *80*, 199.
- [27] A. Rizzo, T. Helgaker, K. Ruud, A. Barszczewicz, M. Jaszuński, P. Jørgensen, *J. Chem. Phys.* **1995**, *102*, 8953.
- [28] A. Rizzo, J. Gauss, *J. Chem. Phys.* **2002**, *116*, 869.
- [29] M. C. Caputo, M. B. Ferraro, P. Lazzeretti, *J. Chem. Phys.* **2000**, *112*, 6141.
- [30] S. Coriani, A. Rizzo, K. Ruud, T. Helgaker, *Mol. Phys.* **1996**, *88*, 931.
- [31] M. Pecul, T. Saue, K. Ruud, A. Rizzo, *J. Chem. Phys.* **2004**, *121*, 3051.
- [32] H. Kjær, S. P. A. Sauer, J. Kongsted, *J. Chem. Phys.* **2011**, *134*, 44514.
- [33] F. Jensen, *J. Chem. Theory Comput.* **2006**, *2*, 1360.
- [34] F. Jensen, *Theo. Chem. Acc.* **2010**, *126*, 371.
- [35] S. P. A. Sauer, *Molecular Electromagnetism: A Computational Chemistry Approach*; Oxford University Press: Oxford, **2011**.
- [36] N. F. Ramsey, *Phys. Rev.* **1953**, *91*, 303.
- [37] P. J. Wilson, T. J. Bradle, D. J. Tozer, *J. Chem. Phys.* **2001**, *115*, 9233.
- [38] C. Lee, W. Yang, R. G. Parr, *Phys. Rev. B* **1988**, *37*, 785.
- [39] S. H. Vosko, L. Wilk, M. Nusair, *Can. J. Phys.* **1980**, *58*, 1200.
- [40] A. D. Becke, *J. Chem. Phys.* **1993**, *98*, 5648.
- [41] E. S. Nielsen, P. Jørgensen, J. Oddershede, *J. Chem. Phys.* **1980**, *73*, 6238.
- [42] K. L. Bak, H. Koch, J. Oddershede, O. Christiansen, S. P. A. Sauer, *J. Chem. Phys.* **2000**, *112*, 4173.
- [43] H. Kjær, S. P. A. Sauer, J. Kongsted, *J. Chem. Phys.* **2010**, *133*, 144106.
- [44] H. Kjær, S. P. A. Sauer, J. Kongsted, Y. Y. Rusakov, L. B. Krivdin, *Chem. Phys.* **2011**, *381*, 35.
- [45] S. P. A. Sauer, *J. Phys. B: At. Mol. Opt. Phys.* **1997**, *30*, 3773.
- [46] T. Enevoldsen, J. Oddershede, S. P. A. Sauer, *Theor. Chem. Acc.* **1998**, *100*, 275.
- [47] U. Benedikt, A. A. Auer, F. Jensen, *J. Chem. Phys.* **2008**, *129*, 64111.
- [48] S. P. A. Sauer, W. T. Raynes, *J. Chem. Phys.* **2000**, *113*, 3121.
- [49] P. F. Provasi, G. A. Aucar, S. P. A. Sauer, *J. Chem. Phys.* **2001**, *115*, 1324.
- [50] V. Barone, P. F. Provasi, J. E. Peralta, J. P. Snyder, S. P. A. Sauer, R. H. Contreras, *J. Phys. Chem. A* **2003**, *107*, 4748.
- [51] Y. Yu. Rusakov, L. B. Krivdin, S. P. A. Sauer, E. P. Levanova, G. G. Levkovskaya, *Magn. Reson. Chem.* **2010**, *48*, 633.
- [52] P. F. Provasi, S. P. A. Sauer, *J. Chem. Phys.* **2010**, *133*, 54308.
- [53] E. D. Hedegård, J. Kongsted, S. P. A. Sauer, *J. Chem. Theory. Comput.* **2011**, *7*, 4077.
- [54] DALTON, A Molecular Electronic Structure Program, Release Dalton2011. <http://daltonprogram.org>, **2011**. Accessed on 13 May 2012.
- [55] O. Vahtras, H. Ågren, P. Jørgensen, H. J. Aa. Jensen, S. B. Padkjær, T. Helgaker, *J. Chem. Phys.* **1992**, *96*, 6120.
- [56] T. Helgaker, M. Watson, N. C. Handy, *J. Chem. Phys.* **2000**, *113*, 9402.
- [57] J. E. Peralta, G. E. Scuseria, J. R. Cheeseman, M. J. Frisch, *Chem. Phys. Lett.* **2003**, *375*, 452.
- [58] W. Deng, J. R. Cheeseman, M. J. Frisch, *J. Chem. Theory. Comput.* **2006**, *2*, 1028.
- [59] R. D. Wigglesworth, W. T. Raynes, S. P. A. Sauer, J. Oddershede, *Mol. Phys.* **1997**, *92*, 77.
- [60] R. D. Wigglesworth, W. T. Raynes, S. P. A. Sauer, J. Oddershede, *Mol. Phys.* **1998**, *94*, 851.
- [61] S. P. A. Sauer, C. K. Møller, H. Koch, I. Paidarová, V. Špirko, *Chem. Phys.* **1998**, *238*, 385.
- [62] S. Kirpekar, S. P. A. Sauer, *Theor. Chem. Acc.* **1999**, *103*, 146.
- [63] M. Grayson, S. P. A. Sauer, *Mol. Phys.* **2000**, *98*, 1981.
- [64] S. P. A. Sauer, W. T. Raynes, R. A. Nicholls, *J. Chem. Phys.* **2001**, *115*, 5994.
- [65] P. F. Provasi, S. P. A. Sauer, *J. Chem. Theory Comput.* **2006**, *2*, 1019.
- [66] A. Yachmenev, S. N. Yurchenko, I. Paidarová, P. Jensen, W. Thiel, S. P. A. Sauer, *J. Chem. Phys.* **2010**, *132*, 114305.
- [67] J. E. Del Bene, I. Alkorta, J. Elguero, *J. Chem. Theory Comput.* **2008**, *4*, 967.
- [68] J. E. Del Bene, I. Alkorta, J. Elguero, *J. Chem. Theory Comput.* **2009**, *5*, 208.
- [69] R. D. Wigglesworth, W. T. Raynes, S. Kirpekar, J. Oddershede, S. P. A. Sauer, *J. Chem. Phys.* **2000**, *112*, 3735.
- [70] R. D. Wigglesworth, W. T. Raynes, S. Kirpekar, J. Oddershede, S. P. A. Sauer, *J. Chem. Phys.* **2001**, *114*, 9192.

Received: 30 November 2011
Revised: 3 April 2012
Accepted: 19 April 2012
Published online on 23 May 2012